JOURNAL OF CATALYSIS 145, 235–238 (1994)

NOTE

XPS Evidence of Alloying in Pd/ZnO Catalysts

Several catalytic studies have dealt with ZnO-supported Pd catalysts, in which the reducible ZnO support is shown to modify the well-known catalytic properties of Pd in hydrogenation. Ryndin *et al.* (1) reported catalytic results for the $CO+H_2$ reaction and established that, among several Pd catalysts supported on various oxides, Pd/ZnO exhibits the highest selectivity toward methanol formation. Recently, this catalyst has been reported to be active in vapour phase ester hydrogenation (2) as well as in selective hydrogenation of 1,3-butadiene (3). The catalytic performance of other ZnO-supported platinum metals (Pt (4, 5); Rh (6)) were also tested in the water–gas shift reaction and in CO hydrogenation, respectively. In these various reactions, which were mostly hydrogenations, metal–support interaction as a result of the reducing pretreatments or of the reaction conditions themselves was claimed to be the crucial factor in all cases.

The physical characterization of the catalysts mentioned above indicated that, while the reducibility of ZnO, an *n*-type semiconductor having interstitial Zn atoms or Zn^+ ions, itself is very limited (7, 8), in the presence of a platinum metal its extent can become significant. In the case of Pt/ZnO catalysts, relying primarily on the results of XRD and XPS investigations, formation of Pt–Zn alloys was proven after reduction at 500–570 K (4, 5, 9, 10). Similar conclusions were drawn for Rh/ZnO catalysts, too (6, 8).

Results on the surface characterization of Pd/ZnO have been published by two research groups. On the basis of the binding energy shift observed for the Pd $3d_{5/2}$ XPS transition, Wehner *et al.* (2, 11) suspected the formation of a Pd–Zn alloy. However, they failed to prove its existence by XRD even in a sample containing 5 m/m% Pd. On the other hand, Hong *et al.* (12) clearly detected the PdZn intermetallic phase by XRD but they did not confirm this result by XPS providing surface information on the electronic states. Although there are XPS data available for various Pd alloys (13–15), no suitable reference data can be found for the Pd–Zn system in the literature.

The main objective of the present note is to provide XPS evidence for alloying taking place during the reduction of a Pd/ZnO catalyst. For this purpose a Pd/ZnO catalyst was reduced at two different temperatures: first at 420 K, which is high enough to reduce Pd completely but at which the formation of the Pd hydride phase as well as that of a Pd-Zn alloy can be avoided; second, at 880 K in order to make the alloy formation complete and to have crystallites large enough for XRD detection. For the sake of comparison pure ZnO and the Pd/ZnO catalyst in "as-prepared" states were also investigated by XPS.

Our sample of 8.5 m/m% Pd content was prepared by mechanical mixing of air-pretreated ZnO (Kadox 25) and PdO powder prepared from $Pd(NO_3)_2$. The sample was reduced in atmospheric flowing H_2 at 420 K for 0.5 h and then 880 K for 0.5 h. Powder diffractograms ($CuK\alpha_1$, λ = 0.15405 nm) were recorded in a Guinier camera equipped with a curved quartz monochromator. The XPS measurements were carried out with a Kratos ES-300 type ESCA machine having a small reactor chamber for in situ reduction of the samples. During the analysis the hemispherical analyser worked in the fixed retarding ratio (F.R.R.) mode and the base pressure did not exceed 10^{-6} Pa. The spectra were generated by the $AlK_{\alpha 1,2}$ X-ray line ($h\nu$ = 1486.67 eV). For the XPS measurements the samples were painted from a mixture of acetone and water onto a cleaned copper stub (no lines of copper could be detected). The binding energy (B.E.) scale was referenced to the Zn $2p_{3/2}$ XPS transition of 1022.00 eV B.E. (3, 8, 15) as an internal standard. During data processing inelastic (Shirley-type) background was subtracted and pseudo-Voigtian curves were used for the peak synthesis in all cases. The reliability of the peak positions so obtained was found to be within 0.10 eV and that of the peak widths (full width at half maximum = FWHM) within 0.05 eV.

The results of the XRD measurements are presented in Fig. 1. As is clearly represented by the lines of Pd(111) and (200) in the 40°–50° region of 2θ, the XRD pattern recorded after the reduction at 420 K displays diffraction lines originating from the metallic Pd phase (12). Besides these, only the pattern of the support ZnO can be found. On the subsequent reduction at 880 K, however, all the lines of Pd metal have disappeared, as shown in Fig. 1b. Here, several new features can be discerned, the majority of which can be attributed to the PdZn intermetallic phase (3, 12). Some very weak lines can also be ob-

0021-9517/94 $5.00

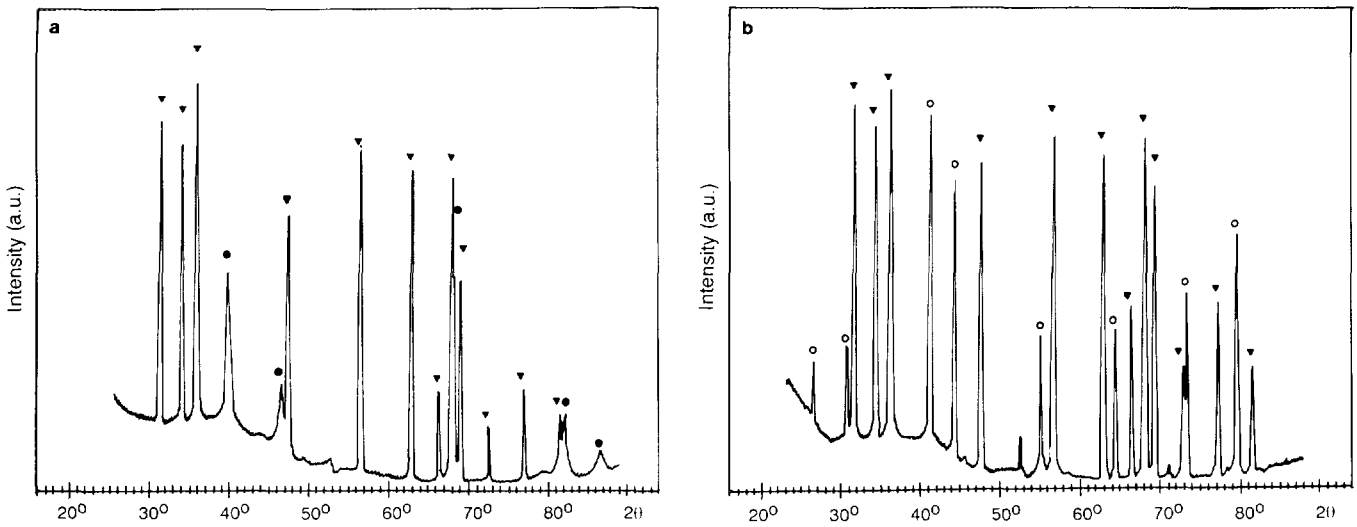

FIG. 1. X-ray powder diffractograms for the 8.5 m/m% Pd/ZnO catalyst after treatments in H_2 at (a) 420 K for 0.5 h (a) and subsequently (b) 880 K for 0.5 h. (▼, ZnO; ●, Pd^0; ○, PdZn).

served, but there is no evidence available for their unambiguous assignation. Nevertheless, it is established that XRD has proved Pd to be present in the metallic phase after reduction at 420 K and mainly in the PdZn intermetallic phase after reduction at 880 K.

Using the Zn $2p_{3/2}$ XPS transition as a binding energy reference at 1022.00 eV B.E., the Zn $3p_{3/2}$ and the Zn $3d_{5/2}$ peaks were found at 88.80 and at 10.10 eV B.E., respectively (spin–orbit coupling: 23.10, 3.00, and 0.85 eV; FWHM: 1.89, 2.85, and 1.47 eV, respectively) in all cases. The value of the Auger parameter (α'(15)) was 2010.25 eV. With the samples (ZnO and Pd/ZnO) in the "as-prepared" state the C 1*s* peaks were located at around 285.2 eV B.E., which is characteristic of hydrocarbon residues (15). Their intensity decreased rapidly following the reduction treatments but the peak shifted to 284.5 eV B.E., which is characteristic of hydrocarbon fragments, only after the reduction at 880 K. This suggests that the original carbonaceous residues are not released or decomposed completely over ZnO on the treatment at 420 K.

Further results obtained by XPS are presented in Table 1 as well as in Fig. 2. The peak of the O 1*s* transition consisted always of two components. The main peak component was found at 530.65–530.70 eV B.E., which is characteristic of transition metal oxides (15), while the other component shifted 1.65–1.55 eV toward higher binding energies. The appearance of the latter component cannot be attributed to differential charging since the other peaks of the XPS spectrum do not contain components in a similar position. On the basis of its binding energy value this second component can be assigned to surface OH groups ($[Zn–OH]_s$) (16). Their presence may be due to the sample preparation for XPS and they remained or formed during the treatments. Although the O 1*s* binding energy of the O^- ion (17) can be found in the same range, its detection may be ruled out because of its relatively low concentration.

Comparing the O 1*s* spectra recorded over the support ZnO and the Pd/ZnO catalyst in the "as-prepared" states the only difference is in the relative contents of the surface OH groups, which may be attributed to some difference in the preparation of the sample for XPS. As can clearly be observed in Fig. 2 the Pd $3d_{5/2}$ spectrum also consists of two components in the "as-prepared" state. The component of lower binding energy can be assigned to zerovalent Pd though its position is slightly lower than that of bulk Pd metal reported in the literature (15). The other component is shifted 1.60 eV toward higher binding energies which corresponds with that of PdO (18). The appearence of Pd^0 in the "as-prepared" sample may be attributed to the partial decomposition of the starting material PdO under UHV conditions. Obviously, it also means that the surface of the particles containing Pd is enriched in zerovalent atoms, i.e., the real extent of the decomposition of PdO is lower than is displayed by the corresponding relative intensity presented in Table 1.

As a result of the H_2 treatment at 420 K the position of the peak characteristic of O^{2-} did not change but its width decreased slightly. The overall O 1*s* intensity referred to that of the Zn $2p_{3/2}$ transition also remained unchanged but the relative concentration of the surface OH groups increased. Simultaneously, PdO disappeared completely while the peak representing Pd^0 was found in its previous position and it was slightly broadened. These changes are accompanied by a significant increase of Pd $3d_{5/2}$/Zn $2p_{3/2}$

TABLE 1

XPS Results for ZnO and Pd/ZnO Samples after Different Treatments

	O 1s[a]			Pd $3d_{5/2}$[b]			
	P1		P2	P1			P2
	B.E. / (eV) R	Width / (eV)	Shift / (eV) R2(%)	B.E. / (eV) R	Width / (eV)	API / (eV)	Shift / (eV) R2(%)
ZnO	530.70	1.45	1.65	—			—
	0.52		32				
Pd/ZnO	530.65	1.49	1.65	334.85	1.19	663.05[c]	1.60
	0.52		27	0.46			56
+ 420 K, H_2	530.65	1.41	1.55	334.85	1.25	662.70	—
	0.53		32	0.59			
+ 880 K, H_2	530.65	1.43	1.55	335.85	1.31	662.85	—
	0.47		18	0.27			

Note. Symbols: P1, P2, peak components; Shift, B.E. shift from the other peak component; Width, FWHM; R, XPS intensity ratio of a given peak (component) referred to that of the Zn $2p_{3/2}$ transition; R2, ratio of P2 in the overall intensity of O 1s and Pd $3d_{5/2}$ transitions, respectively; API, Auger parameter (α'(Pd MNN, Pd $3d_{5/2}$)) of P1.

[a] Auger parameter (O KLL, O 1s), α' = 1040.1 eV.

[b] Spin–orbit coupling: 5.26 ± 0.02 eV.

[c] On the basis of the centroid of the small, very broad Pd LMM line.

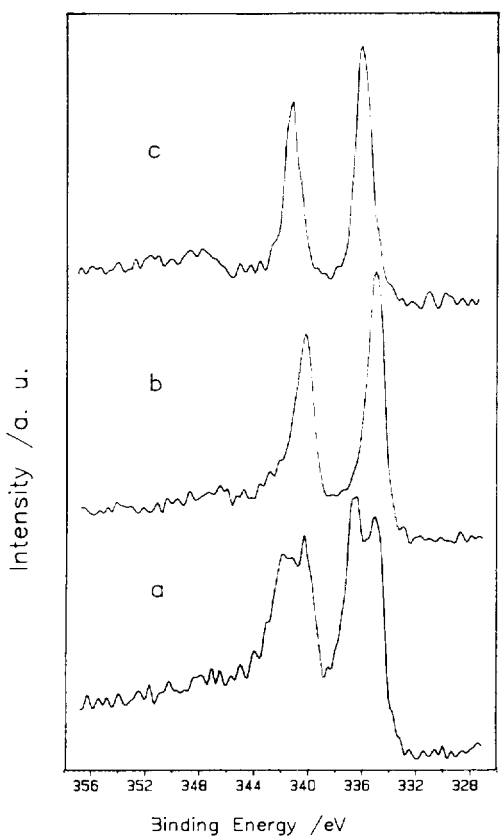

FIG. 2. Pd $3d_{5/2}$ XPS transitions for 8.5 m/m% Pd/ZnO catalyst in the "as-prepared" state (a) and after treatments in H_2 at 420 K for 0.5 h (b) and then at 880 K for 0.5 h (c).

intensity ratio. This latter result may be explained primarily by the increase of the intensity of the Pd $3d_{5/2}$ peak due to the complete reduction of the large particles of PdO into Pd^0 whereby the concentration of the latter in the XPS sampling depth ($d \gg 3\lambda$) increased. Nevertheless, simultaneous coalescence and spreading of the Pd^0 particles over the support surface as was described by Hong *et al.* (12) might also contribute to the increase of the intensity ratio in question. It is more interesting, however, that the overall O 1s/Zn $2p_{3/2}$ intensity ratio, despite the obvious decrease of oxygen due to the reduction of PdO, which is also confirmed by the decrease of the width of the main O 1s peak, remained unchanged. This apparently means that on the hydrogen treatment at 420 K the oxygen/zinc ratio increased in the surface of the ZnO support which must primarily be due to the relative decrease of zinc. At this temperature it cannot be a result of the sublimation of Zn^0 atoms possibly formed but rather to the migration of interstitial zinc ions or atoms (7) into Pd^0 particles which can then spread over them. This result confirms the conception of surface changes in Pd/ZnO catalysts developed by Hong *et al.* (12) on the basis of TEM observations and also supports the idea proposed by Juszczyk and Karpinski relating to the first stage of Pd–Si alloy formation in the Pd/SiO_2 system (19). In addition the relative increase of the surface OH concentration is worth mentioning since it is a direct evidence of the Pd^0-assisted transformation (H-spillover) of ZnO into $[Zn–OH]_s$ as an initial step of its complete reduction.

The subsequent reduction in H_2 at 880 K resulted in no change in the character of the surface oxygen; only its overall concentration together with that of the OH groups decreased significantly. However, in the case of palladium, beside the drastic decrease in the relative intensity, the Pd $3d_{5/2}$ peak slightly further broadened and shifted 1.00 eV toward higher binding energies. These changes were also accompanied by a small 0.15 eV shift of the Auger parameter. A shoulder of the Zn LMM Auger transition also appeared which refers to the presence of zerovalent zinc (8). Based upon the results of the XRD measurements it can unambiguously be established that the electronic structure of the PdZn intermetallic phase can be characterized by the XPS features mentioned before. The large positive shift in the Pd $3d_{5/2}$ XPS transition is similar to those obtained for other Pd alloys (14, 15) and is contrary to the significant negative shifts obtained in the cases of Pt–Zn (4) and Rh–Zn (6, 8) alloys. In addition, taking the small changes of the corresponding Auger parameter into account, on the basis of a simple model (20) it can be established that the palladium atoms become electron deficient on alloying with zinc, which clearly demonstrates the unique character of palladium among the platinum metals (21). The slight broadening of the Pd $3d_{5/2}$ peak may also be in correlation with the formation of PdZn intermetallics in respect of a modification of the environment of Pd^0 atoms by the "dilution" with Zn^0. The considerable decrease in the Pd $3d_{5/2}$/Zn $2p_{3/2}$ intensity ratio can also be attributed to this dilution effect which may further be enhanced by the segregation of zinc in the alloy particle (22). Via the enhanced representation of zinc in the XPS spectrum, the alloy formation together with the extensive reduction of the ZnO surface can also provide the explanation for the remarkable decrease of the surface oxygen concentration. The decrease of the relative OH concentration is a strong evidence that the reaction $2[Zn\text{–}OH]_s \rightarrow ZnO + Zn^0 + H_2O$ also proceeds under the conditions applied.

To sum up, clear evidence has been provided for alloy formation in the Pd/ZnO catalyst by the results of XRD and XPS measurements together. The large positive shift found in the XPS measurements points out that the electronic state of metallic Pd is strongly influenced by Zn in the alloy which probably results in an electron deficient state of Pd. Moreover, Pd-assisted formation of $[Zn\text{–}OH]_s$ groups and their direct reaction with each other has also been proven directly by XPS.

ACKNOWLEDGMENTS

This work was financially supported by the Hungarian Academy of Sciences through the Grant OTKA 1887 and by the US–Hungarian Joint Research Project (JF 183).

REFERENCES

1. Ryndin, Yu. A., Hicks, R. F., Bell, A. T., and Yermakov, Yu. I., *J. Catal.* **70,** 287 (1981).
2. Wehner, P. S., and Gustafson, B. L., *J. Catal.* **135,** 420 (1992).
3. Sárkány, A., Zsoldos, Z., Furlong, B., Hightower, J. W., and Guczi, L., *J. Catal.* **141,** 566 (1993).
4. Li, W., Chen, Y., Yu, C., Wang, X., Hong, Z., and Wei, Z., *in* "Proceedings, 8th International Congress on Catalysis, Berlin, 1984," Vol. 5, p. 205. Verlag Chemie, Weinheim, 1984.
5. Boccuzzi, F., Chiorino, A., Pinna, F., Strukul, G., and Tessari, R., *J. Catal.* **126,** 381 (1990).
6. Ghorai, D. K., Sanyal, R. M., Sen, B., Gosh, S. K., Banerji, K. C., Shpiro, E. S., and Minachev, Kh. M., *React. Kinet. Catal. Lett.* **40,** 259 (1989).
7. Scholten, J. J. F., and van Montfoort, A., *in* "Proceedings, 5th International Congress on Catalysis, Palm Beach, 1972" (J. W. Hightower, Ed.)., Vol. 1, p. 22. North-Holland, New York, 1973.
8. Wehner, P. S., Mercer, P. N., and Apai, G., *J. Catal.* **84,** 244 (1983).
9. Boccuzzi, F., Chiorino, A., and Ghiotti, G., *Surf. Sci.* **209,** 77 (1989).
10. Boccuzzi, F., Ghiotti, G., Chiorino, A., and Marchese, L., *Surf. Sci.* **233,** 141 (1990).
11. Wehner, P. S., Tustin, G. C., and Gustafson, B. L., *J. Catal.* **88,** 246 (1984).
12. Hong, C.-T., Yeh, C.-T., and Yu, F.-H., *Appl. Catal.* **48,** 385 (1989).
13. Martensson, N., Nyholm, R., Calen, H., and Hedman, J., *Phys. Rev. B* **24,** 725 (1981).
14. Steiner, P., and Hufner, S., *Solid State Commun.* **41,** 619 (1982).
15. Briggs, D., and Seah, M. P. (Eds.), "Practical Surface Analysis." Wiley, Chichester, 1983.
16. Wagner, C. D., Riggs, W. N., Davis, L. E., Moulder, J. F., and Muilenberg, G. E. (Eds.), "Handbook of X-ray Photoelectron Spectroscopy." Perkin–Elmer Corp., Physical Electronics Division, Eden Prarie, MN, 1979.
17. Kishi, K., and Roberts, M. W., *J. Chem. Soc. Faraday Trans. I* **71,** 1715 (1975).
18. Légaré, P., Finck, F., Roche, R., and Maire, G., *Z. Phys. D* **12,** 19 (1989).
19. Juszczyk, W., and Karpinski, Z., *J. Catal.* **117,** 519 (1989).
20. Bahl, M. K., Tsai, S. C., and Ghung, Y. W., *Phys. Rev. B* **21,** 1344 (1980).
21. Karpinski, Z., *Adv. Catal.* **37,** 45 (1990).
22. Fasana, A., Abbati, I., and Braikovich, L., *Phys. Rev. B* **26,** 4749 (1982).

Zoltán Zsoldos[1]
Antal Sárkány
László Guczi

Department of Surface Chemistry & Catalysis
Institute of Isotopes of the Hungarian Academy of Sciences
P.O. Box 77, H-1525 Budapest
Hungary

Received December 10, 1992; revised June 16, 1993

[1] E-mail: H903ZSO@ELLA.HU